Trinucleon charge densities and three-nucleon forces

J. L. Friar and B. F. Gibson
Theoretical Division, Los Alamos National Laboratory, Los Alamos, New Mexico 87545

G. L. Payne
Department of Physics and Astronomy, University of Iowa, Iowa City, Iowa 52242

C. R. Chen
Department of Physics and Astronomy, University of Rochester, Rochester, New York 14627
(Received 20 June 1986)

Trinucleon charge densities and charge form factors are calculated in impulse approximation for a large set of wave functions obtained from solving the Faddeev equations for diverse combinations of four two-body force models and three three-nucleon force models. The three-nucleon forces improve the form factor predictions in the region of the secondary maximum slightly, but the experimental data are still substantially higher than the theoretical predictions, while the positions of the theoretical first diffraction minimum and secondary maximum are too high.

I. INTRODUCTION

The behavior of the charge form factor of ^{3}He in the region of the secondary maximum has been a persistent problem for theorists since the data were first taken.[1] In impulse approximation the data are much higher than calculations predict.[2–8] This has led to speculation that exotic mechanisms may be responsible for this behavior. Models which include three-nucleon forces,[2,4–8] pion-exchange currents,[4,5] or explicit quark degrees of freedom[9] have been invoked. In this work we will investigate some aspects of the first of these mechanisms.

The Los Alamos–Iowa collaboration has devoted itself to solving the Faddeev reformulation of the Schrödinger equation in configuration space for bound state eigenvalues and eigenfunctions.[10–13] Faddeev[14] calculations are traditionally organized[8] by expanding the nucleon-nucleon potentials in a series (of infinite extent), each term of which acts only in a single partial wave (e.g., $^1S_0$), truncating the series, and then solving the truncated problem "exactly" in a numerical sense. Until recently, the standard for very accurate calculations was the five-channel problem,[10] keeping all positive-parity partial waves with total angular momentum $j \leq 1$. Hajduk and Sauer[4] extended this to 18 channels (all $j \leq 2$), and recently we developed the first[11] 34-channel solution (all $j \leq 4$). In the (limited) sense that accrual of binding was very small between $j_{\max}=3$ and $j_{\max}=4$, and is estimated to be less than 10 keV for all $j>4$, the "classical" three-nucleon bound-state problem can be said to have been solved. More recently,[12,15] the necessary technical developments were made so that three-body forces (3BF's), those forces[7,16,17] which depend on the simultaneous coordinates of three nucleons, could be included as well.

The result of these calculations is that two-body forces underbind the triton. Realistic nucleon-nucleon forces[18] [Reid soft core (RSC), Paris, super soft core (C) (SSCC), de Tourreil–Rouben–Sprung (B) (TRSB), Argonne V_{14} (AV14)] underbind by roughly 1 MeV. Three-body force models based upon pion exchange provide substantial additional binding, but have a disturbing sensitivity to the short-range behavior. Thus the binding defect can be cured by any of the commonly used 3BF models [Tucson-Melbourne[16] (TM), Brasilian[17] (BR), or Urbana-Argonne[7] (UA)], but the theoretical dependability of this result is problematical.

A number of years ago Fabre de la Ripelle[19] suggested that a remarkable property of most three-body force models[8] could resolve the form factor difficulty as well as the binding problem. These forces, whether classical, atomic, solid state, or nuclear, typically have a strong dependence on the angular orientation of the three interacting particles. Binding prefers equilateral, or near equilateral, configurations, where each particle feels the full attraction of *both* of its neighbors. The charge density, on the other hand, is highly sensitive (in impulse approximation) to other configurations. The charge density, $\rho(r)$, is determined at the origin primarily by medium and large values of q^2 (momentum transfer) in the charge form factor, which are largely negative. Hence, $\rho(0)$ is (experimentally) smaller than calculations predict, because the magnitude of the form factor data in the region of the (negative) secondary maximum lies above the predictions. In the impulse approximation the coordinate r in the charge density corresponds to the distance from the center of mass to one of the protons. Vanishing r corresponds to a collinear configuration of nucleons. It is entirely possible for a 3BF to be attractive in the equilateral configuration and repulsive in the collinear one, thus resolving both binding and form factor problems. Nuclear 3BF models have this qualitative property, but quantitative calculations are clearly necessary.

Many years ago[20] pion-exchange contributions to the charge operator, $\rho_\pi(r)$, were calculated and later applied[5]

to ^{3}He. Effects were found of the requisite sign and sufficient magnitude to resolve the form factor problem. At approximately the same time[21] a more detailed and complete calculation of these operators showed that (1) they are relativistic corrections, (2) they contain important momentum-dependent terms (which have never been included in ^{3}He calculations), (3) they are model dependent,[22] reflecting the physical difference between pseudoscalar and pseudovector couplings of pion and nucleons, and (4) they are ambiguous, reflecting a unitary ambiguity which arises in different methods of calculating these operators. The latter problem is commensural with an identical ambiguity in the relativistic corrections to the one-pion-exchange potential (OPEP);[22] there is no problem at all if the wave functions calculated with a given form of OPEP are used with a commensurate form of the OPE charge operator (such matrix elements will be free of any ambiguity). That is, strength in a matrix element can be shared between the operator and wave functions. The problem is most severe for the isoscalar charge density, where it is possible to *choose* ρ_π to be zero. The exasperating element in this difficulty is that so-called realistic potential models have the wrong form to correspond to *any* of the allowed unitary representations of these operators. Until a complete calculation is performed, no definitive conclusion can be reached. In the work described below we will explore the consequences of a 3BF only in the impulse approximation.

In Sec. II we describe the organization of our impulse approximation charge density calculation, while in the Appendix we discuss the transformation of our wave functions to an L-S basis, which is especially convenient for calculating matrix elements. In Sec. III we discuss our results and in Sec. IV we present our conclusions.

II. CHARGE DENSITY

In the impulse approximation the point-nucleon trinucleon charge density matrix elements have the form

$$\rho(r)=\left\langle \Psi \left| \sum_{i=1}^{A} \hat{\rho}_i \right| \Psi \right\rangle / Z \ , \tag{1}$$

where $\hat{\rho}_i$ is the charge density operator for particle i, Z is the number of protons and A (=3) is the nucleon number. For point nucleons the operators $\hat{\rho}_i$ are given by

$$\hat{\rho}_i=\frac{\delta(r-\frac{2}{3}y_i)}{r^2}\tfrac{1}{2}[1+\tau_3(i)] \ , \tag{2}$$

where $\frac{2}{3}y_i$ is the distance of nucleon i to the trinucleon center of mass and we have normalized the charge density so that

$$\int_0^\infty \rho(r) r^2 dr = 1 \ . \tag{3}$$

For three identical nucleons one can use the symmetry properties of the total wave function to write

$$\rho(r)=3\langle \Psi \,|\, \hat{\rho}_1 \,|\, \Psi \rangle / Z \ . \tag{4}$$

The charge density operator may be separated into an isoscalar and an isovector component, and we define the corresponding charge densities as

$$\rho_s(r)=\left\langle \Psi \left| \frac{\delta(r-\frac{2}{3}y_1)}{r^2} \right| \Psi \right\rangle \tag{5}$$

and

$$\rho_v(r)=3\left\langle \Psi \left| \frac{\delta(r-\frac{2}{3}y_1)}{r^2}\tau_3(1) \right| \Psi \right\rangle \ . \tag{6}$$

We evaluate these matrix elements using a wave function with total isospin $T=\frac{1}{2}$ and with $M_T=\frac{1}{2}$. Therefore, the proton (neutron) density for ^{3}He (^{3}H) is given by

$$\rho_{\{\substack{p\\n}\}}(r)=\tfrac{1}{4}(3\rho_s+\rho_v) \ , \tag{7}$$

and the neutron (proton) density for ^{3}He (^{3}H) is given by

$$\rho_{\{\substack{n\\p}\}}(r)=\tfrac{1}{2}(3\rho_s-\rho_v) \ . \tag{8}$$

The densities ρ_s and ρ_v have the normalizations

$$\int_0^\infty \rho_s r^2 dr = 1 \tag{9}$$

and

$$\int_0^\infty \rho_v r^2 dr = 1 \ . \tag{10}$$

Using the wave function in the form given in Eq. (A26) of the Appendix and averaging over orientations, one can write the matrix element for ρ_s in the form

$$\rho_s(r)=\sum_n \sum_L \frac{1}{2L+1} \sum_{M_L} 8\pi^2[\tfrac{3}{2}]^3 \int_0^\infty x_1^2 dx_1 \int_{-1}^{1} d\mu \,|\, \Psi^n_{LM_L}(x_1,\tfrac{3}{2}r,\mu) \,|^2 \ , \tag{11}$$

where μ is defined by $\hat{\mathbf{x}}_1\cdot\hat{\mathbf{y}}_1=\mu$. Since the isovector density operator has the additional $\tau_3(1)$ operator, the matrix element for ρ_v has the form

$$\rho_v(r)=3\sum_n \sum_{n'} \sum_L \frac{1}{2L+1} \sum_{M_L} 8\pi^2[\tfrac{3}{2}]^3 \int_0^\infty x_1^2 dx_1 \int_{-1}^{1} d\mu \, \Psi^{n'}_{LM_L}(x_1,\tfrac{3}{2}r,\mu)\Psi^{n}_{LM_L}(x_1,\tfrac{3}{2}r,\mu)\langle \phi_{n'} \,|\, \tau_3(1) \,|\, \phi_n \rangle \ . \tag{12}$$

III. CALCULATIONS AND RESULTS

If we ignore isoquartet ($T=\frac{3}{2}$) components of the trinucleon wave function[23] arising from charge-symmetry-breaking elements of the nucleon-nucleon interaction (e.g., the pp Coulomb force), the trinucleon charge densities and charge form factors can be decomposed into isoscalar and isovector components. In the impulse approximation the isovector density has a large component which is simply proportional to the isoscalar

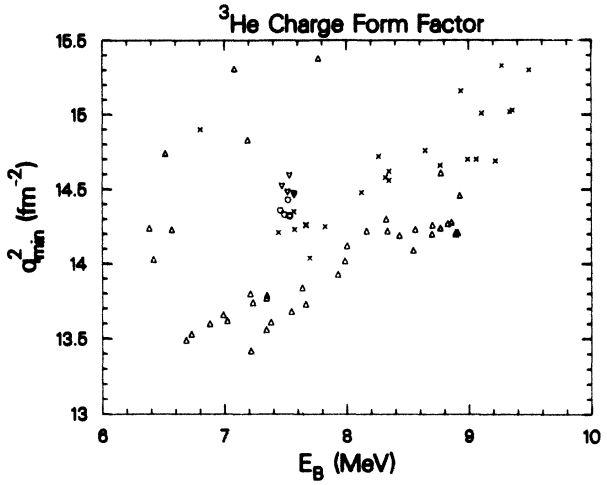

FIG. 1. Position of the first diffraction minimum of the ^{3}He charge form factor, including nucleon finite size, plotted vs the corresponding binding energy for different combinations of two-body and three-body force models. The triangles, $\times$'s, circles, and inverted triangles correspond to the RSC, AV14, SSCC, and TRSB two-body force models.

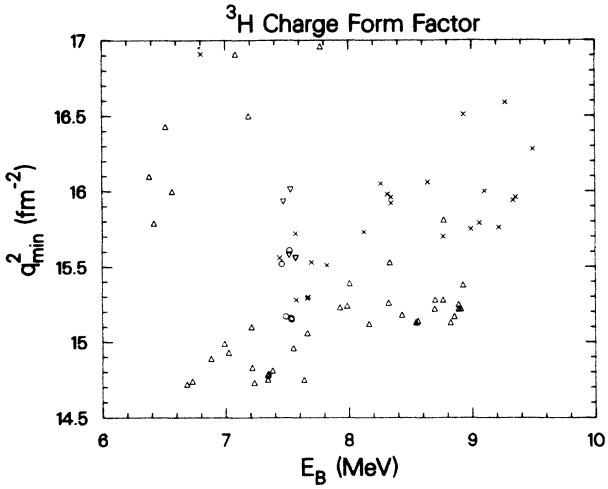

FIG. 2. The ^{3}H case, as in Fig. 1.

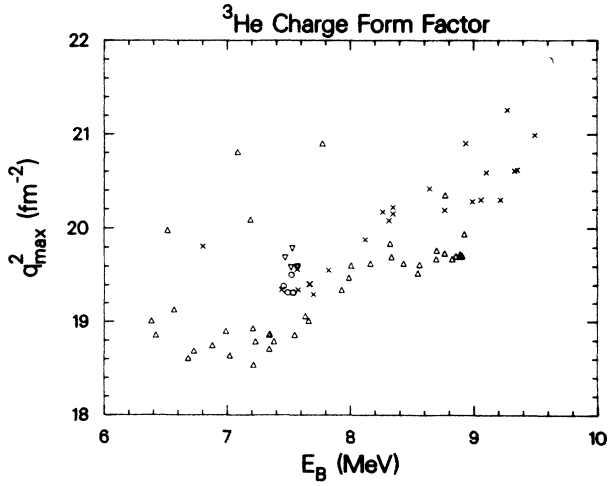

FIG. 3. Position of the secondary diffraction maximum of the ^{3}He charge form factor plotted vs the corresponding binding energy. The data set and symbols are the same as in Fig. 1.

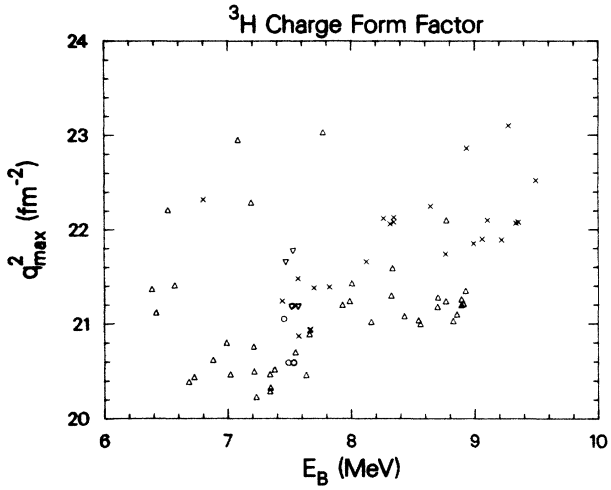

FIG. 4. The ^{3}H case, as in Fig. 3.

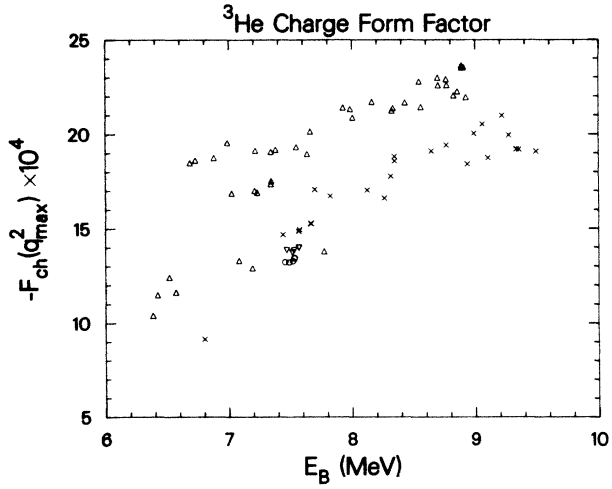

FIG. 5. Size of secondary diffraction maximum of the ^{3}He charge form factor plotted vs the corresponding binding energy. The data set and symbols are the same as in Fig. 1.

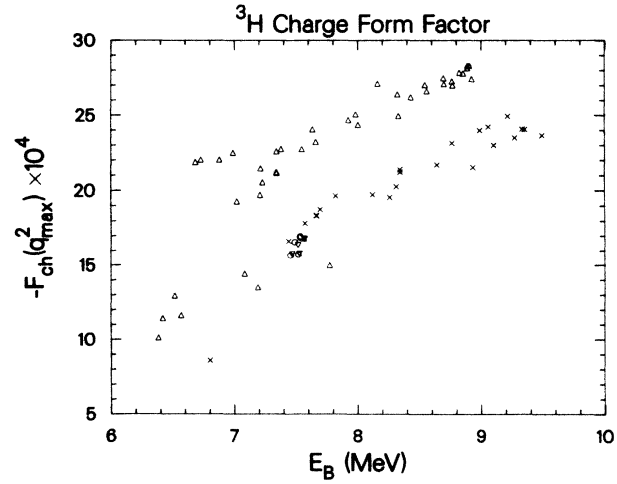

FIG. 6. The ^{3}H case, as in Fig. 5.

one. If that component is subtracted, the remainder determines the difference between the trinucleon charge densities and is denoted by ρ_d. In the impulse approximation *only*, we have

$$\rho_v \equiv \rho_s + 2\rho_d \ , \tag{13a}$$

$$\rho_{^3\mathrm{He}} = \rho_s + \rho_d/2 \ , \tag{13b}$$

$$\rho_{^3\mathrm{H}} = \rho_s - \rho_d \ , \tag{13c}$$

where ρ_d is normalized to zero, and all other densities satisfy $\int \rho(r) r^2 dr = 1$. In earlier work[23,24] one of us[25] adopted an unfortunate notation (ρ_v) for what we call here *(and henceforth)* ρ_d.

The form factors can be calculated easily by Fourier transformation:

$$F(q^2) = \int dr\, r^2 j_0(qr)\rho(r) \ , \tag{14}$$

where j_0 is the usual spherical Bessel function. The effect of the nucleon charge distribution [or form factor, $G_E(q^2)$] can be introduced in the usual way:

$$ZF(q^2) = \tfrac{3}{2} F_s G_E^s \pm \tfrac{1}{2} F_v G_E^v \ , \tag{15}$$

where s and v label isospin components, as before, ($\pm$) refer to ^{3}He and ^{3}H, and $G_E^s = G_E^p + G_E^n, G_E^v = G_E^p - G_E^n$. The nucleon (Sachs) isotopic form factors are normalized to 1; when numerical values are needed, we adopt fit 8.2 of Höhler *et al.*[26]

With the exception of the very-low-q^2 region, determined largely by the various radii, six numbers characterize the trinucleon form factors in the traditional nuclear physics regime ($q^2 < 30$ fm^{-2}). These numbers are the positions of the first diffraction minimum and the secondary diffraction maximum, and the value of the form factor at the latter value of q^2, for both ^{3}He and ^{3}H. The most recent Saclay fits[27] to the world's trinucleon form factor data produce, for ^{3}He,

$$\begin{aligned} q^2_{\min} &= 11.0 \pm 0.7 \text{ fm}^{-2} \ , \\ q^2_{\max} &= 15.65 \text{ fm}^{-2} \ , \\ -F(q^2_{\max}) &= (59 \pm 3) \times 10^{-4} \ , \end{aligned} \tag{16a}$$

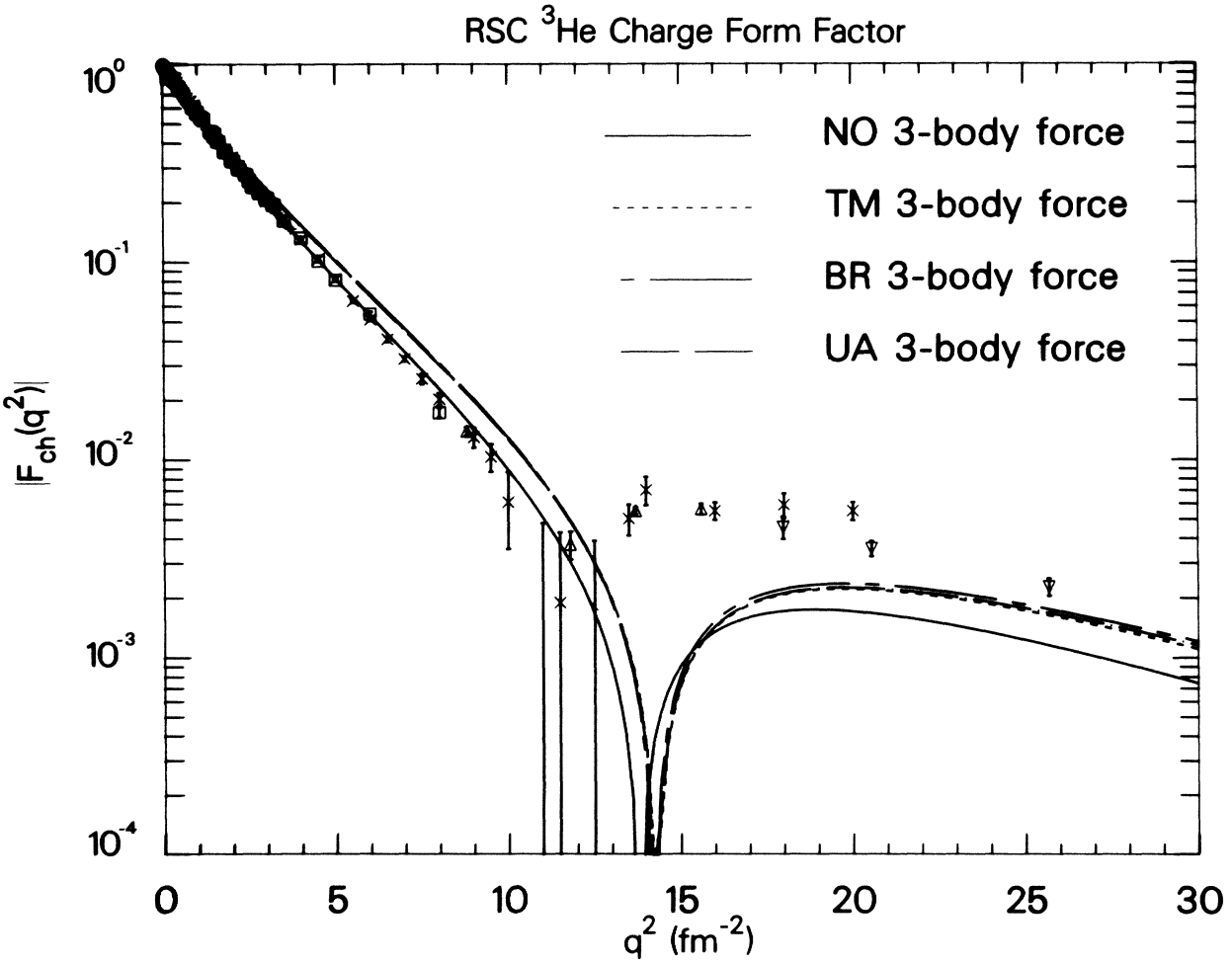

FIG. 7. The magnitude of the RSC ^{3}He charge form factor in the impulse approximation for several three-body force models, plotted versus q^2, together with the experimental data.

and, for ^{3}H,

$$q^2_{\min}=12.6\pm0.5\ \text{fm}^{-2},$$
$$q^2_{\max}=17.25\ \text{fm}^{-2}, \tag{16b}$$
$$-F(q^2_{\max})=(39.5\pm4)\times10^{-4}.$$

For comparison we present our results for these quantities in Figs. 1–6. Nucleon form factors are included in each case. These observables are plotted for each of our wave functions versus the corresponding binding energy E_B. Triangles, $\times$'s, circles, and inverted triangles correspond to RSC, AV14, SSCC, and TRSB two-body potential models, respectively. Three-nucleon forces were added only to the RSC and AV14 models. All points with $E_B>7.7$ MeV contain such a force. A few of these cases include a pp Coulomb force, which has little significance in the results. In every figure there is a band, a clear trend upward with increasing binding energy. Most of those points for small E_B, which lie off the band, correspond to three-channel calculations, which have a severely truncated tensor force, and cannot be said to be particularly realistic for this reason. In each case the AV14 model tends to produce larger values of $q^2_{\min}$ or $q^2_{\max}$ than the RSC model, and smaller values of $|F(q^2_{\max})|$. The positions of all of our minima and maxima are at too large a value of q^2, while the values of the maxima themselves are too small, compared to experiment.

This is shown most clearly in Figs. 7 and 8, which compare our RSC 34-channel results corresponding to several 3BF models with the experimental data.[1,27–29] The various three-nucleon forces clearly increase the value of the secondary maxima and, just as clearly, generate comparable results for this range of momentum transfers. Moreover, there is a serious problem at moderate momentum transfers, which stems from the fact that the diffraction minima are not correctly located. Ironically, the case corresponding to no 3BF fits the low-q^2 data quite well, while adding a 3BF spoils this agreement.

The reason for the change in shape of the form factor curves for small q^2 can be understood as follows. The most obvious quantitative effect of the inclusion of a 3BF is the increase in binding. This affects the exterior part of the wave function[30] in an obvious way: the value of κ in

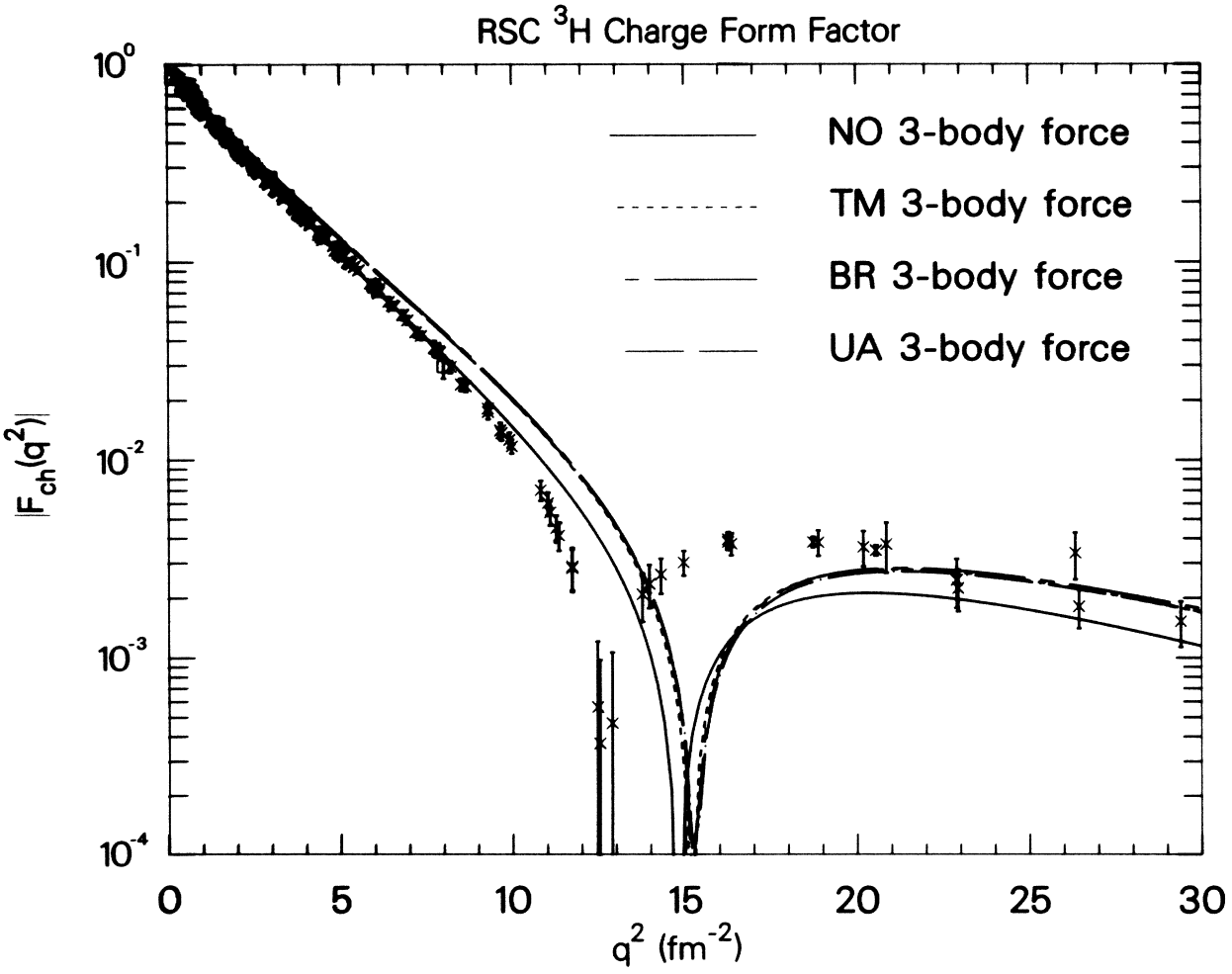

FIG. 8. The magnitude of the RSC ^{3}H charge form factor in the impulse approximation for several three-body force models, plotted vs q^2, together with the experimental data.

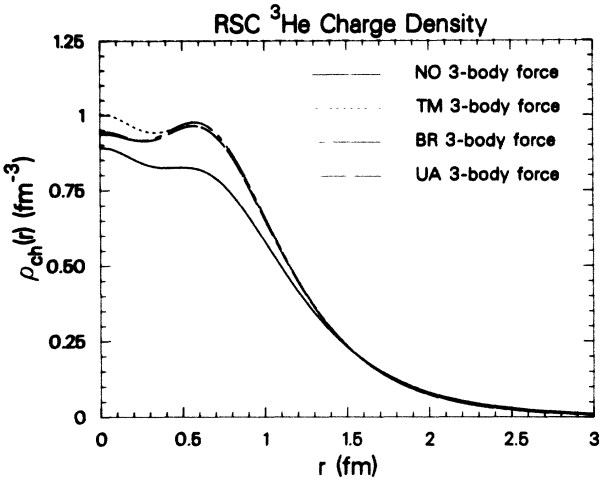

FIG. 9. The RSC ^{3}He charge density in the impulse approximation for several three-body force models, plotted vs r.

Eq. (A8) changes because $\kappa \sim E_B^{1/2}$. We therefore posit (as a model) that the increase in binding simply changes $\Psi^2(\mathbf{x},\mathbf{y})$ (with binding energy E_B^0) to $\Psi^2(\lambda\mathbf{x},\lambda\mathbf{y})$ (with binding energy E_B), where $\lambda \sim (E_B/E_B^0)^{1/2} > 1$. This changes $\rho_{ch}(r)$ to $\lambda^3\rho_{ch}(\lambda r)$, where the multiplicative factor preserves the normalization. Calculating a form factor changes $F_{ch}(q)$ to $F_{ch}(q/\lambda)$, which simply "stretches" the momentum transfer scale of the form factor. This clearly accounts for some of the binding effect in Figs. 7 and 8, but cannot account for the increase in the secondary maximum. The "stretching" model predicts the same value for any secondary maximum, albeit at a shifted value of q^2. A closer examination of the stretching model shows that its predictions are quantitative only at quite small values of q^2, although they are qualitative for substantially larger values of q^2.

Finally, we examine the point-nucleon impulse approximation charge densities shown in Figs. 9 and 10. The ^{3}He charge density has a maximum at the origin when no 3BF is included. This changes to a slight minimum (except for the TM model) for the 3BF cases. The size of this depression is very much smaller than that found by Sick,[31] reflecting the 50% increase in the secondary maximum for our 3BF wave functions, while a factor of 3—4 is needed in order to agree with the data. The form factors for the various 3BF cases in Fig. 7 are nearly the same. The different behavior of the TM case near the origin in Fig. 9 is symptomatic of the differences in the form factors at much larger values of q^2 than those shown in Fig. 7.

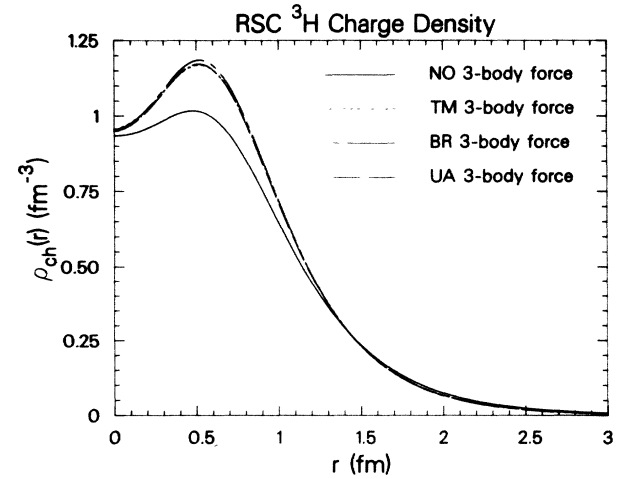

FIG. 10. The RSC ^{3}H charge density in the impulse approximation for several three-body force models, plotted vs r.

The ^{3}H charge density has a small hole for every model, caused by the $L=2$ (D-wave) component of the wave function. This component necessarily has a completely symmetric $S=\frac{3}{2}$ (spin-quartet) wave function. Consequently, the two neutrons in the $L=2$ part of the ^{3}H wave function are forced by the Pauli principle to be in a (relative) odd-parity state, as is the remaining proton. Thus the charge density corresponding to this component must vanish at the origin ($\sim r^2$). There are two protons in ^{3}He, and singling out one of them can leave the remaining neutron and proton in any orbital state, and this places no restriction on $\rho(r)$ for small r. Although it is difficult to observe the effect in Figs. 9 and 10, we note that the increased binding draws in the charge density from large r toward the origin, which is yet another manifestation of the stretching in the form factor.

IV. CONCLUSIONS

The various combinations of two-body and three-body force models that we have discussed above are clearly inadequate to account for the experimental behavior of the trinucleon form factors in the impulse approximation. The experimental (first) diffraction minimum lies at a smaller value of q^2 than the theoretical models predict, as does the position of the secondary maximum. Theoretically, the size of this maximum is too small. Although the inclusion of three-body forces helps increase the size of the secondary maximum, "stretching" of the form factor makes the calculated positions of the minimum and maximum move outward, worsening the disagreement with experiment. Clearly, the physics we have built into our model calculations is inadequate. What remedies for these problems are available?

The *ad hoc* addition to either form factor of a component which vanishes at $q^2=0$ and is negative in the region of the diffraction minimum and secondary maximum would alleviate all of these problems. This negative component would shift the form factor minimum and maximum to smaller values of q^2, and would accentuate the size of the maximum. This simple structural behavior accounts[5] for the helpfulness of the meson-exchange currents. It is obviously difficult for three-body force models to accomplish this in the impulse approximation and to increase the binding at the same time. We mentioned earlier, however, that there was no fundamental difference between certain pion-exchange contributions to the charge operator, ρ_π, and inclusion of relativistic corrections to the two-[21] (and three-[32]) nucleon Hamiltonians, ΔH_π. The matrix elements of the charge operator have a certain strength, which can be dialed from the

operator ρ_π into the wave functions via ΔH_π in an arbitrary manner. Those *ad hoc* calculations of ρ_π which have been heretofore performed have a negative sign and an appropriate strength to alleviate some of the problems in Figs. 7 and 8, however.

For this reason it is imperative that a trinucleon calculation be performed which (at least) includes relativistic corrections. One would, of course, prefer a model calculation with the minimal correct physics which avoids a $(v/c)^2$ expansion. Only in this way will we be able to make a clear statement about relativistic effects and their role in the ^{3}He and ^{3}H form factors.

The work of J.L.F. and B.F.G. was performed under the auspices of the U.S. Department of Energy, while that of C.R.C. and G.L.P. was supported in part by that agency.

APPENDIX

The configuration space Schrödinger wave function is expressed as the sum of the three Faddeev amplitudes[10] ψ_i. That is, one writes

$$\Psi(\mathbf{x}_1,\mathbf{y}_1)=\psi(\mathbf{x}_1,\mathbf{y}_1)+\psi(\mathbf{x}_2,\mathbf{y}_2)+\psi(\mathbf{x}_3,\mathbf{y}_3) \equiv\psi_1+\psi_2+\psi_3 , \tag{A1}$$

where we use the center-of-mass Jacobi variables

$$\mathbf{x}_i=\mathbf{r}_j-\mathbf{r}_k \tag{A2a}$$

and

$$\mathbf{y}_i=\tfrac{1}{2}(\mathbf{r}_j+\mathbf{r}_k)-\mathbf{r}_i . \tag{A2b}$$

The $\mathbf{r}_i$ are the coordinates of particle i, and the subscripts are to be taken cyclically. The total wave function can be expressed as a function of any pair of the Jacobi variables. We choose to use the pair $(\mathbf{x}_1,\mathbf{y}_1)$, which are conventionally written as $(\mathbf{x},\mathbf{y})$. The other two pairs can be expressed in terms of $\mathbf{x}_1$ and $\mathbf{y}_1$, by the relations

$$\mathbf{x}_2=-\tfrac{1}{2}\mathbf{x}_1+\mathbf{y}_1 , \tag{A3a}$$

$$\mathbf{y}_2=-\tfrac{3}{4}\mathbf{x}_1-\tfrac{1}{2}\mathbf{y}_1 \tag{A3b}$$

and

$$\mathbf{x}_3=-\tfrac{1}{2}\mathbf{x}_1-\mathbf{y}_1 , \tag{A4a}$$

$$\mathbf{y}_3=\tfrac{3}{4}\mathbf{x}_1-\tfrac{1}{2}\mathbf{y}_1 . \tag{A4b}$$

For each of the Faddeev amplitudes we use the partial-wave expansion in the j-J coupling scheme. Thus we write

$$\psi(\mathbf{x}_i,\mathbf{y}_i)=\sum_\alpha \frac{\phi_\alpha(x_i,y_i)}{x_i y_i}\,|\alpha\rangle_i , \tag{A5}$$

where we have introduced the reduced partial-wave function ϕ_α, and the $|\alpha\rangle_i$ are the angular momentum and spin-isospin functions for the channel α and the variables $(\hat{\mathbf{x}}_i,\hat{\mathbf{y}}_i)$. That is,

$$|\alpha\rangle_i=|[(l_\alpha,s_\alpha)j_\alpha,(\ell_\alpha,S_i)J_\alpha]JM;(t_\alpha,T_i)TM_T\rangle , \tag{A6}$$

and l_α is the relative orbital angular momentum of particles j and k, s_α is the spin angular momentum of particles j and k, j_α is the total angular momentum of particles j and k, ℓ_α is the orbital angular momentum of particle i relative to the center of mass of particles j and k, S_i is the spin of particle i ($S_i=\frac{1}{2}$), J_α is the total angular momentum of particle i, J is the total angular momentum of the three-particle system, t_α is the total isospin of particles j and k, T_i is the isospin of particle i ($T_i=\frac{1}{2}$), and T is the total isospin of the three-particle system.

The 34 j-J partial-wave states that we have used for our largest calculations are given in Ref. 13. The reduced wave functions are expressed in terms of the hyperspherical variables, defined by

$$x_i=\rho\cos\theta_i \tag{A7a}$$

and

$$y_i=\frac{\sqrt{3}}{2}\rho\sin\theta_i . \tag{A7b}$$

We write

$$\phi_\alpha(x_i,y_i)=F_\alpha(\rho,\theta_i)\frac{e^{-\kappa\rho}}{\rho^{1/2}} , \tag{A8}$$

where κ is the bound-state wave number. The binding energy is given by

$$E_B=\frac{\hbar^2\kappa^2}{M} . \tag{A9}$$

It is the $F_\alpha(\rho,\theta_i)$ which form the eigenfunctions corresponding to our Faddeev eigenvalues. The $F_\alpha(\rho,\theta_i)$ are expanded in bicubic splines on a rectangular grid in the ρ-θ_i coordinates:

$$F_\alpha(\rho,\theta_i)=\sum_{m=1}^{M}\sum_{n=1}^{N} a^\alpha_{mn}s_m(\rho)s_n(\theta_i) , \tag{A10}$$

where $s_m(\rho)$ and $s_n(\theta_i)$ are the cubic Hermite splines.[33] The Faddeev equations are reduced to a matrix eigenvalue problem for the eigenvalue κ and the eigenvectors whose components are the a^α_{mn}. Given the a^α_{mn} and κ, one can use Eqs. (A1), (A5), (A8), and (A10) to construct the total wave function for any values of $\mathbf{x}_1$ and $\mathbf{y}_1$.

While the j-J coupling scheme is convenient for solving the Faddeev equations, it is not the most convenient scheme for using the wave functions to calculate matrix elements. For most numerical calculations it is preferable to separate the orbital angular momentum wave function from the spin-isospin wave function. To do this we first transform the channel functions $|\alpha\rangle_i$ to the L-S coupling scheme and use the relations

$$|\alpha\rangle_i=\sum_{L,S}[(2j_\alpha+1)(2J_\alpha+1)(2L+1)(2S+1)]^{1/2}\begin{Bmatrix} l_\alpha & s_\alpha & j_\alpha \\ \ell_\alpha & S_i & J_\alpha \\ L & S & J \end{Bmatrix}|[(l_\alpha,\ell_\alpha)L,(s_\alpha,S_i)S]JM;(t_\alpha,T_i)TM_T\rangle_i . \tag{A11a}$$

Defining the L-S channel states

$$|\beta\rangle_i = |[(l_\beta,\ell_\beta)L_\beta,(s_\beta,S_i)S_\beta]JM;(t_\beta,T_i)TM_T\rangle_i \ , \tag{A11b}$$

one can write Eq. (A11) in the form

$$|\alpha\rangle_i = \sum_\beta c_{\alpha\beta}|\beta\rangle_i \ , \tag{A12}$$

where the L-S states are given in Ref. 13.

Using Eq. (A12), we can now rewrite Eq. (A5) as

$$\psi(\mathbf{x}_i,\mathbf{y}_i) = \sum_\beta \sum_\alpha c_{\alpha\beta}\frac{\phi_\alpha(x_i,y_i)}{x_i y_i}|\beta\rangle_i = \sum_\beta \frac{\phi_\beta(x_i,y_i)}{x_i y_i}|\beta\rangle_i \ . \tag{A13}$$

Using Eqs. (A8) and (A10), one finds

$$\phi_\beta(x_i,y_i) = \sum_\alpha c_{\alpha\beta}F_\alpha(\rho,\theta_i)\frac{e^{-\kappa\rho}}{\rho^{1/2}} = F_\beta(\rho,\theta_i)\frac{e^{-\kappa\rho}}{\rho^{1/2}} \ . \tag{A14}$$

We have introduced

$$F_\beta(\rho,\theta_i) = \sum_\alpha c_{\alpha\beta}\sum_{m=1}^{M}\sum_{n=1}^{N} a^\alpha_{mn}s_m(\rho)s_n(\theta_i) = \sum_{m=1}^{M}\sum_{n=1}^{N} b^\beta_{mn}s_m(\rho)s_n(\theta_i) \ , \tag{A15}$$

where the new expansion coefficients b^β_{mn} are defined by

$$b^\beta_{mn} = \sum_\alpha c_{\alpha\beta}a^\alpha_{mn} \ . \tag{A16}$$

Using the expansion coefficients b^β_{mn} one can combine Eqs. (A13)—(A15) to construct the Faddeev amplitudes in the L-S representation. The total wave function is still the sum of the three Faddeev amplitudes.

Both the j-J and the L-S partial-wave expansions defined above contain spin-isospin functions for three nucleons coupled to all permutations. For the evaluation of matrix elements which contain spin and isospin operators, we choose to rewrite the wave function in terms of spin-isospin functions formed by first coupling particles 2 and 3 together and then coupling to particle 1 to form the total spin and isospin. For three nucleons with spins $S_1=S_2=S_3=\frac{1}{2}$ and isospins $T_1=T_2=T_3=\frac{1}{2}$, we define the state functions

$$\chi_n = |[(S_2,S_3)s_n,S_1]S_nM_S\rangle \equiv |(s_n,S_1)S_n\rangle \ , \tag{A17}$$

and

$$\eta_n = |[(T_2,T_3)t_n,T_1]T_nM_T\rangle \equiv |(t_n,T_1)T\rangle \ . \tag{A18}$$

The three possible spin states are

$$\chi_1 = |[0,\tfrac{1}{2}]\tfrac{1}{2}\rangle \ , \tag{A19a}$$

$$\chi_2 = |[1,\tfrac{1}{2}]\tfrac{1}{2}\rangle \ , \tag{A19b}$$

$$\chi_3 = |[1,\tfrac{1}{2}]\tfrac{3}{2}\rangle \ . \tag{A19c}$$

Since we consider only states with a total isospin of $\frac{1}{2}$, the two possible isospin states are

$$\eta_1 = |[0,\tfrac{1}{2}]\tfrac{1}{2}\rangle \tag{A20a}$$

and

$$\eta_2 = |[1,\tfrac{1}{2}]\tfrac{1}{2}\rangle \ . \tag{A20b}$$

Following Schiff,[34] we choose as our spin-isospin basis states linear combinations of the states defined in (A19) and (A20). These states are

$$\phi_0 = \frac{1}{\sqrt{2}}(\chi_2\eta_1-\chi_1\eta_2) \ , \tag{A21a}$$

$$\phi_1 = \frac{1}{\sqrt{2}}(\chi_1\eta_1-\chi_2\eta_2) \ , \tag{A21b}$$

$$\phi_2 = -\frac{1}{\sqrt{2}}(\chi_1\eta_2+\chi_2\eta_1) \ , \tag{A21c}$$

$$\phi_3 = -\chi_3\eta_2 \ , \tag{A21d}$$

$$\phi_4 = \chi_3\eta_1 \ , \tag{A21e}$$

$$\phi_5 = \frac{1}{\sqrt{2}}(\chi_1\eta_1+\chi_2\eta_2) \ . \tag{A21f}$$

Our spin-isospin states, χ and η, are not the same as Schiff's,[34] but we have defined the ϕ's to be the same as those of Schiff and Gibson.[35]

The L-S channel states can be written in the form

$$|\beta\rangle_i = \sum_{M_L,M_S}(L_\beta M_L S_\beta M_S|JM)[Y_{l_\beta}(\hat{\mathbf{x}}_i)\otimes Y_{\ell_\beta}(\hat{\mathbf{y}}_i)]_{L_\beta M_L}|(s_\beta,S_i)S_\beta M_S;(t_\beta,T_i)TM_T\rangle_i \ . \tag{A22}$$

The spin-isospin state function can be rewritten as linear combinations of the ϕ's defined in Eq. (A21). We write

$$|(s_\beta,S_i)S_\beta M_S;(t_\beta,T_i)TM_T\rangle_i = \sum_n d^{(i)}_{\beta n}\phi_n \ . \tag{A23}$$

Now each of the Faddeev amplitudes can be written in the form

$$\psi(\mathbf{x}_i,\mathbf{y}_i) = \sum_n\sum_\beta\sum_{M_L}\sum_{M_S}(L_\beta M_L S_n M_S|JM)d^{(i)}_{\beta n}\frac{\phi_\beta(x_i,y_i)}{x_i y_i}[Y_{l_\beta}(\hat{\mathbf{x}}_i)\otimes Y_{\ell_\beta}(\hat{\mathbf{y}}_i)]_{L_\beta M_L}\phi_n \ . \tag{A24}$$

The total wave function can now be written in the form

$$\Psi(\mathbf{x},\mathbf{y})=\sum_n\sum_\beta\sum_{M_L}\sum_{M_S}(L_\beta M_L S_n M_S\,|\,JM)\left\{d^{(1)}_{\beta n}\frac{\phi_\beta(x_1,y_1)}{x_1y_1}[Y_{l_\beta}(\hat{\mathbf{x}}_1)\otimes Y_{\ell_\beta}(\hat{\mathbf{y}}_1)]_{L_\beta M_L}\right.$$
$$+d^{(2)}_{\beta n}\frac{\phi_\beta(x_2,y_2)}{x_2y_2}[Y_{l_\beta}(\hat{\mathbf{x}}_2)\otimes Y_{\ell_\beta}(\hat{\mathbf{y}}_2)]_{L_\beta M_L} \tag{A25}$$
$$\left.+d^{(3)}_{\beta n}\frac{\phi_\beta(x_3,y_3)}{x_3y_3}[Y_{l_\beta}(\hat{\mathbf{x}}_3)\otimes Y_{\ell_\beta}(\hat{\mathbf{y}}_3)]_{L_\beta M_L}\right\}\phi_n\ .$$

Collecting the terms with same value of L_β, one can write the total wave function in the form

$$\Psi(\mathbf{x},\mathbf{y})=\sum_n\sum_L\sum_{M_L}\sum_{M_S}(LM_L S_n M_S\,|\,JM)\Psi^n_{LM_L}(\mathbf{x},\mathbf{y})\phi_n\ , \tag{A26}$$

where the $\psi^n_{LM_L}$ can be constructed from the spline expansion and the appropriate spherical harmonics. This decomposition is virtually identical to the bipolar harmonic expansion advocated in Ref. 36.

[1]J. S. McCarthy, I. Sick, R. R. Whitney, and M. R. Yearian, Phys. Rev. Lett. **25**, 884 (1970); J. S. McCarthy, I. Sick, and R. R. Whitney, Phys. Rev. C **15**, 1396 (1977); R. G. Arnold *et al.*, Phys. Rev. Lett. **40**, 1429 (1978).

[2]T. Sasakawa, H. Okuno, and T. Sawada, Phys. Rev. C **23**, 905 (1981); T. Sasakawa and T. Sawada, *ibid.* **19**, 2035 (1979); T. Sasakawa, A. Fukunaga, and S. Ishikawa, invited talk at Third International Symposium on Mesons and Nuclei, Bechyne, Czechoslovakia (1985) [Czech. J. Phys. B **36**, 312 (1981)].

[3]J. L. Friar, B. F. Gibson, E. L. Tomusiak, and G. L. Payne, Phys. Rev. C **24**, 665 (1981). This work contains many references to older work.

[4]Ch. Hajduk and P. U. Sauer, Nucl. Phys. **A369**, 321 (1981); Ch. Hajduk, P. U. Sauer, and W. Streuve, *ibid.* **A405**, 581 (1983).

[5]E. Hadjimichael, R. Bornais, and B. Goulard, Phys. Rev. Lett. **48**, 583 (1982); Phys. Rev. C **27**, 831 (1983).

[6]W. Glöckle, Nucl. Phys. **A381**, 343 (1982).

[7]J. Carlson, V. R. Pandharipande, and R. B. Wiringa, Nucl. Phys. **A401**, 59 (1983); R. B. Wiringa, *ibid.* **A401**, 86 (1983).

[8]J. L. Friar, B. F. Gibson, and G. L. Payne, Annu. Rev. Nucl. Sci. **34**, 403 (1984); J. L. Friar, in *New Vistas in Electronuclear Physics* (Plenum, New York, 1986).

[9]J. P. Vary, S. A. Coon, and H. J. Pirner, in *International Conference on Hadronic Probes and Nuclear Interactions,* Tempe, AZ, March 11–14, 1985, AIP Conf. Proc. No. 133, edited by J. Comfort *et al.* (AIP, New York, 1985), p. 83.

[10]G. L. Payne, J. L. Friar, B. F. Gibson, and I. R. Afnan, Phys. Rev. C **22**, 823 (1980).

[11]C. R. Chen, G. L. Payne, J. L. Friar, and B. F. Gibson, Phys. Rev. C **31**, 2266 (1985).

[12]C. R. Chen, G. L. Payne, J. L. Friar, and B. F. Gibson, Phys. Rev. Lett. **55**, 374 (1985); Phys. Rev. C **33**, 1740 (1986).

[13]C. R. Chen, Ph.D. thesis, University of Iowa, 1985 (unpublished).

[14]L. D. Faddeev, Zh. Eksp. Teor. Fiz. **39**, 1429 (1960) [Sov. Phys.—JETP **12**, 1014 (1961)].

[15]T. Sasakawa and S. Ishikawa, Few Body Sys. **1**, 3 (1986).

[16]S. A. Coon, M. D. Scadron, P. C. McNamee, B. R. Barrett, D. W. E. Blatt, and B. H. J. McKellar, Nucl. Phys. **A317**, 242 (1979).

[17]H. T. Coelho, T. K. Das, and M. R. Robilotta, Phys. Rev. C **28**, 1812 (1983).

[18]R. V. Reid, Ann. Phys. (N.Y.) **50**, 411 (1968); B. D. Day, Phys. Rev. C **24**, 1203 (1981), provides the higher partial waves; M. Lacombe, *et al.*, *ibid.* **21**, 861 (1980); R. de Tourreil and D. W. L. Sprung, Nucl. Phys. **A201**, 193 (1973); R. de Tourreil, B. Rouben, and D. W. L. Sprung, *ibid.* **A242**, 445 (1975); R. B. Wiringa, R. A. Smith, and T. L. Ainsworth, Phys. Rev. C **29**, 1207 (1984).

[19]M. Fabre de la Ripelle, C. R. Acad. Sci. (Paris) **288**, 325 (1979).

[20]W. M. Kloet and J. A. Tjon, Phys. Lett. **49B**, 419 (1974).

[21]J. L. Friar, Ann. Phys. (N.Y.) **104**, 380 (1977); Phys. Lett. **59B**, 145 (1975).

[22]J. L. Friar and B. F. Gibson, Phys. Rev. C **15**, 1779 (1977).

[23]G. L. Payne, J. L. Friar, and B. F. Gibson, Phys. Rev. C **22**, 832 (1980).

[24]J. L. Friar, B. F. Gibson, E. L. Tomusiak, and G. L. Payne, Phys. Rev. C **24**, 665 (1981).

[25]J. L. Friar, Nucl. Phys. **A156**, 43 (1970).

[26]G. Höhler *et al.*, Nucl. Phys. **B114**, 505 (1976).

[27]F.-P. Juster *et al.*, Phys. Rev. Lett. **55**, 2261 (1985); S. Platchkov and B. Frois, private communication.

[28]J. M. Cavedon *et al.*, Phys. Rev. Lett. **49**, 986 (1982); P. C. Dunn *et al.*, Phys. Rev. C **27**, 71 (1983); G. A. Retzlaff and D. M. Skopik, *ibid.* **29**, 1194 (1984); C. R. Otterman *et al.*, Nucl. Phys. **A436**, 688 (1985).

[29]H. Collard *et al.*, Phys. Rev. **138**, B57 (1965); D. H. Beck, J. Asai, and D. M. Skopik, Phys. Rev. C **25**, 1152 (1982); D. H. Beck *et al.*, *ibid.* **30**, 1403 (1984); D. H. Beck, private communication.

[30]J. L. Friar, B. F. Gibson, C. R. Chen, and G. L. Payne, Phys. Lett. **161B**, 241 (1985).

[31]I. Sick, in *Lecture Notes in Physics* (Springer, Berlin, 1978), Vol. 87, p. 236.

[32]S. A. Coon and J. L. Friar, Phys. Rev. C (in press).

[33]P. M. Prenter, *Splines and Variational Methods* (Wiley, New York, 1975).

[34]L. I. Schiff, Phys. Rev. **133**, B802 (1964).

[35]B. F. Gibson and L. I. Schiff, Phys. Rev. **138**, B26 (1965); B. F. Gibson, Nucl. Phys. **B2**, 501 (1967).

[36]J. L. Friar, E. L. Tomusiak, B. F. Gibson, and G. L. Payne, Phys. Rev. C **24**, 677 (1981).